Journal of Applied Polymer Science

Effects of facile amine-functionalization on the physical properties of epoxy/graphene nanoplatelets nanocomposites

Mihye Seong, Dae Su Kim
Department of Chemical Engineering, Chungbuk National University, 1 Chungdaero, Seowongu, Cheongju Chungbuk 362-763, Korea
Correspondence to: D. S. Kim (E-mail: dskim@cbnu.ac.kr)

ABSTRACT: Graphene nanoplatelets (GNPs) have excellent thermal, electrical, and mechanical properties. The incorporation of GNPs into a polymer can remarkably enhance the thermal and mechanical properties of the polymer especially when GNPs are well dispersed in the polymer matrix with strong interfacial bonding. Therefore, in this study, GNPs were amine-functionalized by covalently bonding 4,4′-methylene dianiline onto their surfaces via a facile synthetic route. The amine-functionalization was confirmed by FTIR spectroscopy and TGA. Epoxy/GNPs nanocomposites were prepared and their curing behavior, thermomechanical properties and impact strength were investigated. The amine-functionalization increased curing rate, storage modulus, thermal dimensional stability, and impact strength of the nanocomposites. The SEM images for the fracture surface of the nanocomposite with amine-functionalized GNPs showed a smooth and ductile failure-like surface, resulted from the improved interfacial bonding between GNPs and the epoxy matrix. © 2015 Wiley Periodicals, Inc. J. Appl. Polym. Sci. **2015**, *132*, 42269.

KEYWORDS: composites; graphene and fullerenes; properties and characterization; thermosets

Received 11 December 2014; accepted 25 March 2015
DOI: 10.1002/app.42269

INTRODUCTION

There have been growing interests in incorporating nanoparticles (nanospheres, nanotubes, nanorods, nanoplatelets, etc.) into a polymer matrix to enhance various properties such as thermal stability, mechanical properties, and flame retardancy.[1–5] Recently, some studies have been focused on enhancing the mechanical properties of epoxy resins through the incorporation of reinforcing nanoparticles.[6–8]

Epoxy resin is a representative thermoset that polymerizes when mixed with a curing agent like amines and anhydrides. They are extensively used in many industrial fields including coatings, adhesives, insulating materials, and composite materials because of their excellent thermomechanical properties, chemical resistance, and adhesion properties.[9] In the field of composite materials, to make high performance epoxy nanocomposites, graphene nanoplatelets (GNPs) have been used as carbon nanofillers because they have excellent inherent thermal and mechanical properties.[10–12]

GNPs have a stacked plate structure with several graphene monolayers stacked together and each monolayer generally called graphene consists of only aromatic carbon atoms covalently bonded each other in honeycomb crystal lattice.[13,14] They have attracted a lot of interests as nanofillers in making composites because they have low price, high electrical conductivity, and excellent mechanical and thermal properties.[15] They have potential benefits when used as nanofillers in composites because they can enhance physical properties significantly even at a very small loading.[16] Also the advantages derived from exfoliated morphology include much higher glass transition temperature and stiffness due to polymer chain confinement effects resulting from the enormous surface area of overall monolayer graphene nanosheets incorporated.[17] However, due to the thermodynamically unstable enormous surface area and strong van der Waals forces and phi–phi stacking forces between layers, GNPs usually tend to exist as reaggregate and stack[18]. So, it is very difficult to produce an epoxy nanocomposite with exfoliated morphology having each monolayer graphene nanosheet dispersed independently and homogeneously in the epoxy matrix.[19]

For a better performance, the epoxy nanocomposites with GNPs require a homogeneous dispersion of GNPs as well as a strong interfacial bonding between GNPs and the epoxy matrix.[20] Thus, to maximize improvements in the composites' properties, functionalized GNPs with enhanced compatibility to the epoxy resins have been developed.[21–23] An effective surface functionalization of GNPs, which improves the interfacial interactions between the inorganic GNPs and a polymer matrix to facilitate

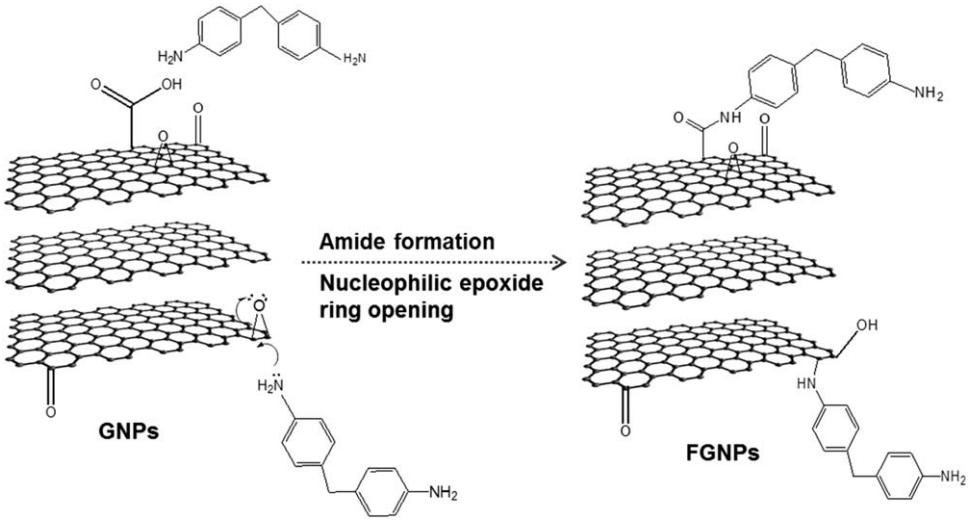

Figure 1. The reaction scheme to prepare the amine-functionalized graphene nanoplatelets.

the effective interfacial stress transfer from the polymer to the GNPs, prevents aggregation and promotes the dispersion of GNPs in the polymer matrix.[24] Therefore, the incorporation of functionalized GNPs into an epoxy resin could surely enhance the thermal and mechanical properties of the epoxy resin significantly.[25]

There are two ways in functionalizing the surfaces of inorganic nanoparticles like graphene and GNPs. The first is achieved through noncovalent coupling to the surfaces with small molecules like silane coupling agents and the second is based on covalently grafting organic molecules with functional groups onto the surfaces through reaction between the functional groups of the organic molecules and the functional groups of the nanoparticles' surfaces. The advantage of the second way over the first is that the organic molecule-grafted nanoparticles are much more effective in improving composites' properties and can be designed with the desired properties.[24] The two ways could be applied at the same time by noncovalently wrapping the surfaces of monolayer graphene nanosheets with a surfactant and then covalently functionalizing the wrapped surfaces by treatment with aryl diazonium salts.[26]

In our previous study, high-performance epoxy nanocomposites with amine-functionalized monolayer graphene nanosheets were synthesized.[27] However, the amine-functionalization of monolayer graphene nanosheets needed a lot of efforts with low yield. Therefore, in this study, a facile synthetic route to covalently bond aromatic diamine molecules onto GNPs' surfaces was used and the effects of the facile amine-functionalization on the curing behavior, thermomechanical properties, impact strength and fracture surface morphology of epoxy/GNPs nanocomposites were investigated.

EXPERIMENTAL

Materials

A diglycidyl ether of bisphenol-A (DGEBA)-type epoxy resin (YD-128 from Kuk Do Chem., Korea) and an aromatic amine curing agent, 4,4′-methylene dianiline (MDA from Sigma-Aldrich) were used to formulate a neat epoxy resin system. The epoxy equivalent weight of YD-128 was about 185 g/mol and the viscosity was 12,000 cP at 25°C. GNPs with oxidized surfaces (xGnP-M-5 from XG science Corp.) were used as reinforcing carbon nanofillers. The thickness and diameter of the GNPs were 6–8 nm and 5 μm, respectively. MDA was also used to amine-functionalize the GNPs' surfaces.

Preparation of Amine-Functionalized GNPs

Amine-functionalized GNPs (named FGNPs in this study) were synthesized by covalently bonding MDA molecules onto the GNPs' oxidized surfaces through both amide formation with carboxylic groups and nucleophilic substitution with epoxide groups as shown in Figure 1.[28–30]0.5 g of the original GNPs was suspended in 200 mL of tetrahydrofuran (THF) by sonication.[31] Then, after adding 0.5 g of MDA, the suspension that was immersed in an oil bath at 80°C was refluxed under N_2 atmosphere for 6 h. The resulting amine-functionalized GNPs were washed with ethanol five times, then filtered and dried at 40°C in a vacuum oven for 24 h.

Preparation of Epoxy/GNPs Nanocomposites

The original or amine-functionalized GNPs (0.5–1.5 phr (parts per hundreds of the DGEBA resin)), except for the curing agent to prevent premature curing reaction, were mixed with the DGEBA resin by sonication at 60°C for 1 h, then the curing agent was added by stoichiometry and mixed further by sonication for 30 min. The nanocomposite mixture was poured into a mold and cured in an oven at 100°C for 2 h, 180°C for 1 h and 200°C for 30 min. For comparison, a neat epoxy resin sample without GNPs was also prepared by the same mixing and curing procedure.

Measurements

Spectroscopy. To confirm the amine-functionalization of the original GNPs, a Fourier-transform infrared spectroscopy (Nicoret IR200, Thermo Scientific Co. USA) was used. The original and functionalized GNPs were mixed with KBr powder, respectively, and disc shape specimens were prepared for FTIR

analysis. The FTIR spectra of the original and functionalized GNPs were obtained in the wavenumber range of 4000–500 cm^{-1}.

Thermal Analysis. To confirm the amine-functionalization of the original GNPs, a thermogravimetric analyzer (SDT 2960, TA Instruments, New Castle, DE, USA) was also used. Each measurement was carried out under N_2 atmosphere from room temperature to 600°C at a heating rate of 20°C/min.

To investigate the curing behavior of the epoxy/GNPs nanocomposite systems, a differential scanning calorimeter (DSC 2910, TA Instruments) was used. About 10 mg of each uncured sample was placed in a hermetic aluminum pan, and tested immediately after sealing and positioning it right on the DSC sample cell. Each sample was cured dynamically at 10°C/min under N_2 atmosphere from room temperature to 300°C.

To investigate the dynamic mechanical properties of the epoxy/GNPs nanocomposites, a dynamic mechanical analyzer (DMA 2940, TA Instruments) was used. The specimens were subjected to a sinusoidal displacement of 20 μm at a frequency of 1 Hz under a static loading force of 0.05 N. The scanning rate was 3°C/min from room temperature to 300°C. The dimensions of each specimen were 36 × 12.8 × 3.2 mm.

To investigate the thermal expansion properties of the epoxy/GNPs nanocomposites, a thermomechanical analyzer (TMA 2940, TA Instruments) was used. The heating rate was 3°C/min from room temperature to 300°C.

Impact Test. The un-notched izod impact test was performed at room temperature using an impact tester (SJI-103, Sung Jin Co., Seoul, Korea) according to ASTM D256. The dimensions of each specimen were 50 × 13 × 4 mm. An average value of at least 6 specimens' impact strength data was reported for accuracy.

Morphology

A field emission scanning electronic microscope (FE-SEM, LEO-1530FE, Carl Zeiss NTS GmbH, Oberkochen, Germany) was used to investigate the morphology of the fracture surfaces of the epoxy/GNPs nanocomposites. The surfaces of the nanocomposites were coated with Pt by sputtering for 5 min prior to the FE-SEM observation.

RESULTS AND DISCUSSION

Characterization of Amine-Functionalized GNPs

A direct evidence for the successful grafting of MDA molecules onto the GNPs' surfaces could be provided by FTIR analysis as shown in Figure 2. The GNPs have oxidized surfaces with functional groups like epoxy, carbonyl, and hydroxyl groups. Thus, the IR spectrum of the GNPs shows the absorption peak at about 1700 cm^{-1} for the stretching vibrations of C═O groups and the absorption peak at about 3500 cm^{-1} for the stretching vibrations of O—H groups. The IR spectrum of the FGNPs also shows the absorption peak at about 1700 cm^{-1} for the stretching vibrations of C═O groups. Compared to the original GNPs, the amine-functionalized GNPs (FGNPs) exhibited the IR absorption peaks caused by the amine-functionalization. The absorption peaks at 3440 cm^{-1} are attributed to the N—H

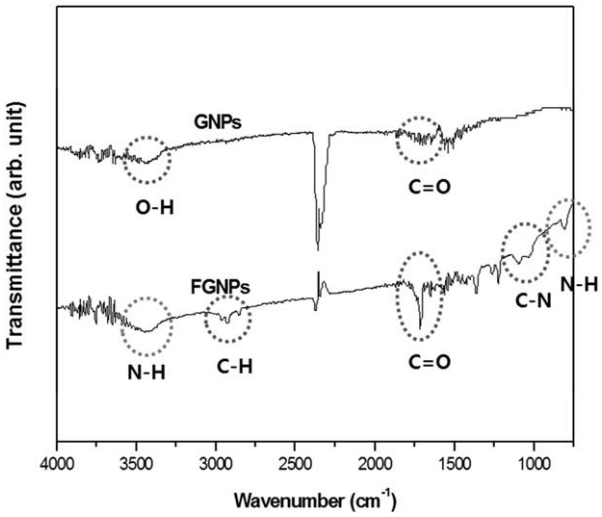

Figure 2. FTIR spectra of the original and amine-functionalized GNPs.

stretching vibrations of the amine groups of MDA. The other peaks at 665 cm^{-1} are caused by the N—H wagging of MDA. Moreover, the additional absorption peaks at 2860–2924 cm^{-1} provide an evidence for the amine-functionalization because they should be assigned to C—H stretching vibrations of MDA. The other absorption peak at 1100 cm^{-1} correspond to the C—N stretching vibrations of amide groups, which were formed by chemical reaction between the surface carboxyl groups of the original GNPs and the amine groups of MDA. These results confirm the amine-functionalization of the original GNPs.

The TGA curves for the original and amine-functionalized GNPs and MDA are shown in Figure 3. The TGA curve for MDA shows that the decomposition (evaporation) of the MDA molecules starts at about 200°C and ends at about 330°C. From this result, the significant thermal decomposition (9.9% weight decrease) of the FGNPs observed between 220 and 380°C was considered due to the thermal decomposition of the MDA molecules covalently bonded to the surfaces of the GNPs. It was considered that, compared to the free MDA molecules, the thermal decomposition of the MDA molecules covalently bonded to

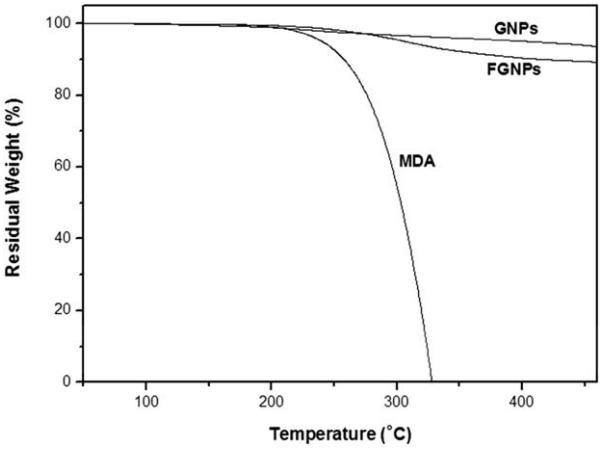

Figure 3. TGA curves of the original and amine-functionalized GNPs and MDA.

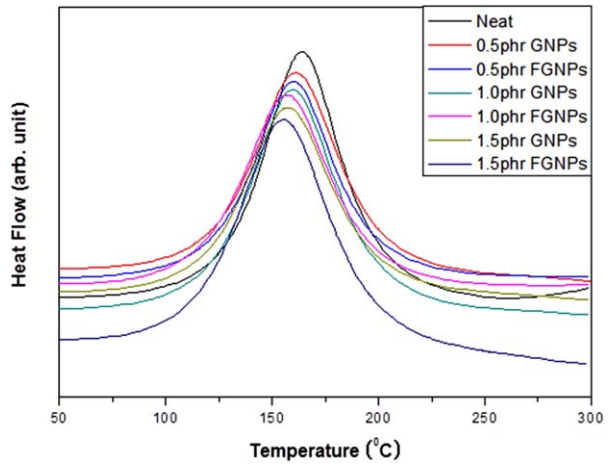

Figure 4. Dynamic DSC thermograms showing the curing behavior of each system with different GNPs or FGNPs loadings. [Color figure can be viewed in the online issue, which is available at wileyonlinelibrary.com.]

the surfaces of the GNPs retarded up to the higher temperature region because they were covalently bonded to the surfaces of the GNPs.

From both the FTIR and TGA data, it could be confirmed that MDA molecules were successfully covalently bonded to the surfaces of the original GNPs via the facile synthetic route.

Curing Behavior of Epoxy/GNPs Nanocomposites

The effects of both GNPs content and amine-functionalization on the curing behavior of the epoxy/GNPs nanocomposites were investigated by dynamic DSC method as shown in Figure 4. The exothermic DSC curve shifted to a lower temperature region with increasing the original GNPs content. The exothermic peak temperatures are listed in Table I. The GNPs were efficient in accelerating the curing process of the epoxy matrix, reducing significantly the time needed for complete curing at the same curing condition. The GNPs have a few hydroxyl groups and these can accelerate the curing of epoxide rings with amines. Moreover, since the GNPs have higher thermal conductivity than the epoxy matrix, they would help easier and faster heat supply from external heat sources during dynamic curing, making the epoxy matrix cure faster.

Addition to the positive effects of the GNPs on the epoxide curing described above, the FGNPs have a few amine groups, originated from MDA molecules covalently bonded to their surfaces, which can directly react with epoxide groups in the matrix resin. As shown in Figure 4, the addition of the FGNPs into the epoxy resin showed considerable peak shift to a lower temperature region, indicating a faster curing.

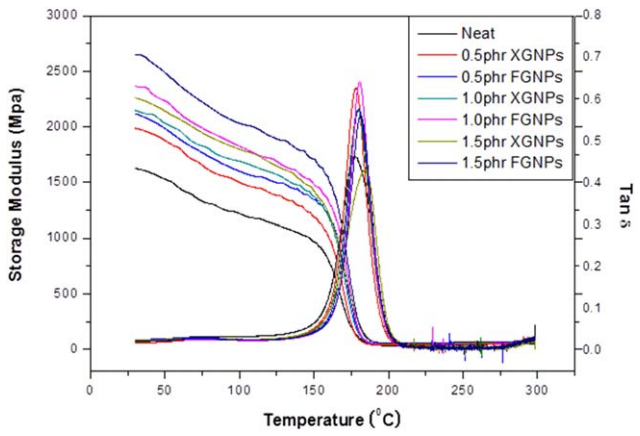

Figure 5. DMA thermograms showing the storage modulus and tan δ values of the epoxy nanocomposites. [Color figure can be viewed in the online issue, which is available at wileyonlinelibrary.com.]

Thermomechanical Properties of Epoxy/GNPs Nanocomposites

Figure 5 shows the storage modulus (E') and loss factor (tan δ) change with temperature for the neat epoxy resin and the epoxy nanocomposites with the GNPs or the FGNPs. Table I lists the DMA data (E' and T_g) for each sample. The storage modulus of the epoxy/GNPs nanocomposites increased with increasing the GNPs content because of the intrinsic high modulus of the rigid GNPs. Similarly, the glass transition temperature (T_g) determined by taking the temperature of the tan δ maximum also increased with increasing the GNPs content. The increase in T_g with increasing the GNPs content can be attributed to the increased restriction of chain segmental mobility caused by the chain confinement effect of the GNPs. As listed in Table I, the storage moduli of the epoxy nanocomposites with 1.5 phr of the FGNPs or the GNPs were 2650 (62.9% increase compared to the modulus (1627 MPa) of the neat epoxy) and 2260 MPa (38.9% increase compared to the modulus of the neat epoxy), respectively. The reason why the epoxy/FGNPs nanocomposites showed superior storage moduli compared to the epoxy/GNPs nanocomposites could be explained in terms of improved interfacial bonding between the FGNPs and the epoxy matrix due to the amine-functionalization. The nanocomposites with the FGNPs 1.5 phr showed slightly lower T_g compared to the nanocomposites with the same amount of the GNPs. This suggests that the FGNPs act as reactive plasticizers, when added over 1.0 phr, that reduce slightly the cross-linking density of the cured epoxy matrix, thus improving slightly the flexibility of chain segments of the cross-linked epoxy matrix.[32,33]

It is noteworthy that compared to the storage modulus (2447 MPa) at 30°C of the epoxy/functionalized monolayer graphene nanosheets nanocomposite in our previous study[27] that (2370 MPa) of the epoxy/FGNPs nanocomposite in this study is slightly lower at the same carbon nanofiller content of 1 phr. The T_g (217.1°C) of the nanocomposite in the previous study is considerably higher than that (180.7°C) of the epoxy/FGNPs nanocomposite in this study because in the case of the nanocomposite with functionalized monolayer graphene nanosheets, both the confinement effect and the improved interfacial bond strength effect would be significant.

The coefficients of linear thermal expansion (CLTE) of the nanocomposites were measured by taking longitudinal dimension chance with temperature between 50°C and 150°C and listed in Table I. The CLTEs of the nanocomposites measured below their T_gs decreased with increasing the GNPs or the FGNPs content. The addition of the GNPs or the FGNPs to the

Table I. Physical Properties of the Epoxy Nanocomposites with the GNPs or the FGNPs

Sample	T_{max}[a] (°C)	E'[b] (MPa)	T_g[c] (°C)	CLTE[d] (10^{-6} m m^{-1} K^{-1})	Impact strength (J/m)
Neat	164.2	1627	177.4	67.4	43.5±1.9
0.5 phr GNPs	161.5	1988	177.9	66.7	54.8±2.1
0.5 phr FGNPs	160.2	2119	179.9	66.0	66.5±3.3
1.0 phr GNPs	159.7	2149	179.3	64.0	74.1±3.1
1.0 phr FGNPs	157.4	2370	180.7	63.0	90.6±4.1
1.5 phr GNPs	158.0	2260	184.4	62.7	80.4±6.4
1.5 phr FGNPs	155.9	2650	181.5	62.5	95.1±6.5

[a] The exothermic peak temperatures of the DSC thermograms.
[b] Storage modulus values determined by the DMA thermograms at 30°C.
[c] T_g determined by taking the temperature of tan δ maximum.
[d] Coefficient of linear thermal expansion obtained from the TMA thermograms between 50°C; and 150°C;.

epoxy matrix would reduce the thermal expansion of the nanocomposites because they have inherently lower thermal expansion characteristics compared to the neat epoxy resin. Furthermore, the confinement effect of the GNPs or the FGNPs would limit the mobility of polymer chains leading to the lower thermal expansion of the nanocomposites. The CLTEs of the epoxy/FGNPs nanocomposites were smaller than those of the epoxy/GNPs nanocomposites at the same loadings because of the improved interfacial bonding between the FGNPs and the epoxy matrix.

To investigate how the amine-functionalization of the original GNPs affects the toughness of the epoxy nanocomposites comprising them, the unnotched izod impact test was carried out. Figure 6 and Table I show the impact strength data of each nanocomposite together with that of the neat epoxy resin for comparison. As expected, the neat epoxy resin exhibited the lowest impact strength of 43.5 J/m. With increasing the GNPs content, the impact strength of the epoxy/GNPs nanocomposite increased up to 80.4 J/m (84.8% increase compared to the impact strength of the neat epoxy) at 1.5 phr GNPs loading. The nanocomposites with the FGNPs also showed a similar trend with much more increase in impact strength, due to the improved interfacial bonding between the FGNPs and the epoxy matrix, up to 95.1 J/m (118.6% increase compared to the impact strength of the neat epoxy) at 1.5 phr FGNPs loading.

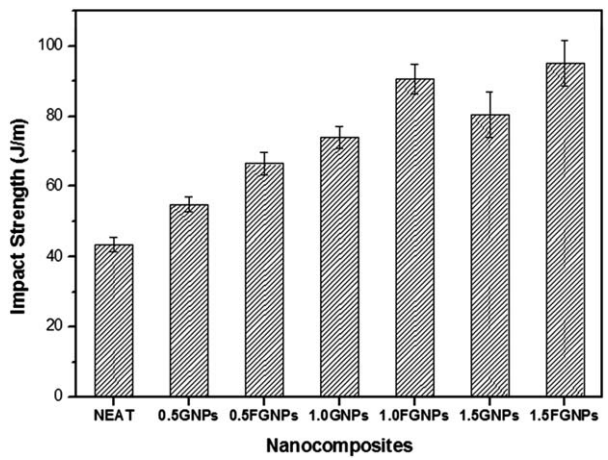

Figure 6. Impact strengths of the epoxy nanocomposites.

Compared to the impact strength (75.1 J/m) of the epoxy/functionalized monolayer graphene nanosheets nanocomposite in our previous study[27] that (90.6 J/m) of the epoxy/FGNPs, nanocomposite in this study is quite higher at the same carbon nanofiller content of 1 phr. This shows that the FGNPs of this study prepared by the facile synthetic route are much better in improving the toughness of the epoxy system though the functionalized monolayer graphene nanosheets were better in improving the modulus and T_g of the epoxy system.

In this study, the storage modulus and impact strength of the epoxy resin could be considerably improved by incorporating the FGNPs which can be covalently bonded to the epoxy matrix via the curing reaction between epoxide groups in the epoxy matrix and amine groups at the FGNPs' surfaces. In general, the main drawback of epoxy resins is their low impact strength caused by their high cross-linking density. When a modifier or filler is added to an epoxy resin to improve impact strength, the resulting material has generally decreased modulus. However, this study showed that the main drawback of an epoxy resin could be covered by incorporating the FGNPs without any negative effects such as decreased modulus.

Morphology of Epoxy/GNPs Nanocomposites

Figure 7 shows the SEM images of the fracture surfaces of the epoxy nanocomposites with 0.5 phr GNPs (a,b) or 0.5 phr FGNPs (c,d), respectively, at two different magnifications. In the case of the nanocomposite with the GNPs, as shown in the SEM image (b), the GNPs could be pulled out from the epoxy matrix due to their poor interfacial bonding to the epoxy matrix. Whereas, in the case of the nanocomposite with the FGNPs, as shown in the SEM image (d), any pull-out of the FGNPs from the epoxy matrix was not observed, indicating that the FGNPs had strong interfacial bonding to the epoxy matrix. Compared to the SEM image (a) for the nanocomposite with the GNPs, the SEM image (c) for the nanocomposite with the

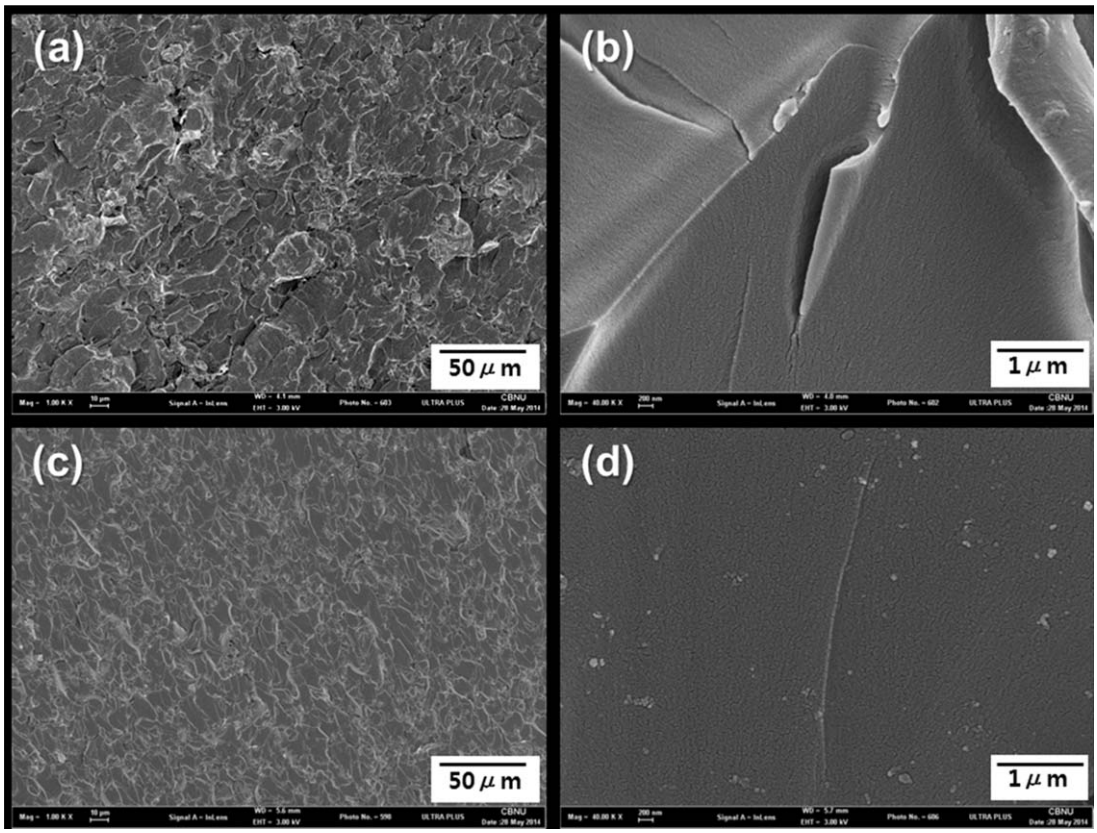

Figure 7. SEM images of the epoxy nanocomposites with (a,b) 0.5 phr GNPs or (c,d) 0.5 phr FGNPs, respectively, at different magnifications.

FGNPs showed a much smoother and ductile failure-like surface, resulted from the improved interfacial bonding between the FGNPs and the epoxy matrix due to the amine-functionalization. This fracture surface image supported the reason why the nanocomposites with the FGNPs showed excellent impact strengths.

CONCLUSIONS

The effects of the facile amine-functionalization of the original GNPs on the physical properties of the epoxy/GNPs nanocomposites were elucidated. The FTIR and TGA data confirmed that the amine-functionalization of the GNPs with 4,4′-methylene dianiline was successful. The curing rate of the epoxy/GNPs nanocomposites increased slightly with increasing GNPs content. The amine-functionalization made the curing rate of the nanocomposites faster. The storage modulus and T_g of the epoxy/GNPs nanocomposite increased with the GNPs content considerably, though the nanocomposite with 1.5 phr FGNPs showed limited T_g increase due to the FGNPs' reactive plasticizer effect. The CLTE value of the nanocomposite decreased with increasing the GNPs or the FGNPs content. The mechanical properties of the nanocomposite with 1.5 phr FGNPs were the best because of the improved interfacial bonding between the FGNPs and the epoxy matrix. The SEM image of the nanocomposite with 0.5 phr FGNPs showed a much smoother and ductile failure-like fracture surface, resulted from the improved interfacial bonding between the FGNPs and the epoxy matrix.

REFERENCES

1. Kumar, S. K.; Krishnamoorti, R. *Annu. Rev. Chem. Biomol. Eng.* **2010**, *1*, 37.
2. Ladhari, A.; Ben Daly, H.; Belhadjsalah, H.; Cole, K. C.; Denault, J. *Polym. Degrad. Stad.* **2010**, *95*, 429.
3. Yuan, Y.; Shi, W. F. *Prog. Org. Coat.* **2010**, *69*, 92.
4. Che, X. C.; Jin, Y. Z.; Lee,Y. S. *Prog. Org. Coat.* **2010**, *69*, 534.
5. Ganesan, V.; Ellison, C. J.; Pryamitsyn, V. *Soft Matter* **2010**, *6*, 4010.
6. Ruiz-Pe'rez, L.; Royston, G. J.; Fairclough, J. P. A.; Ryan, A. J. *Polymer* **2008**, *49*, 4475.
7. Zhu, J.; Peng, H. Q.; Rodriguez-Macias, F.; Margrave, J. L.; Khabashesku,V. N.; Imam, A. M.; Karen, L.; Barrera, E. V. *Adv. Funct. Mater.* **2004**, *14*, 643.
8. Chen, L.; Chai, S.; Liu, K.; Ning, N.; Gao, J.; Liu, Q.; Chen, F.; Fu, Q. *ACS Appl. Mater. Interfaces* **2012**, *4*, 4398.
9. Unnikrishnan, K. P.; Thachil, E. T. *Des. Monomers Polym.* **2006**, *9*, 129.
10. Bortz, D. R.; Heras, E. G.; Gullon, I. M. *Macromolecules* **2012**, *45*, 238.
11. Zaman, I.; Kuan, H. C.; Meng, Q. S.; Michelmore, A.; Kawashima, N.; Pitt, T.; Zhang, L. Q.; Gouda, S.; Luong, L.; Ma, J. *Adv. Funct. Mater.* **2012**, *22*, 2735.
12. Shen, X. J.; Liu, Y.; Xiao, H. M.; Feng, Q. P.; Yu, Z. Z.; Fu, S. Y. *Compos. Sci. Technol.* **2012**, *72*, 1581.

13. Novoselov, K.; Geim, A. K.; Morozov, S.; Jiang, D.; Zhang, Y.; Dubonos, S.; Grigorieva, I.; Firsov, A. *Science* **2004**, *306*, 666.
14. Geim, A. K. *Science* **2009**, *324*, 1530.
15. Zheng, W.; Lu, H.; Wong, S. *J. Appl. Polym. Sci.* **2004**, *91*, 2781.
16. Shen, J. W.; Chen, X. M.; Huang, W. H. *J. Appl. Polym. Sci.* **2003**, *63*, 225.
17. Park, J.; Kim, D. S. *Polym. Eng. Sci.* **2014**, *54*, 969.
18. McAllister, M. J.; Li, J. L.; Adamson, D. H.; Schniepp, H. C.; Abdala, A. A.; Liu, J. *Chem. Mater.* **2007**, *19*, 4396.
19. Verdejo, R.; Bernal, M. M.; Romasanta, L. J.; Lopez-Manchado, M. A. *J. Mater. Chem.* **2011**, *21*, 3301.
20. Byun, J.; Kim, D. S. *Polym. Compos.* **2010**, *31*, 1449.
21. Bao, G.; Guo, Y.; Song, L.; Kan, Y.; QIAN, X.; Hu, Y. *J. Mater. Chem.* **2011**, *21*, 13290.
22. Zaman, I.; Kuan, H. C.; Meng, Q. S.; Michelmore, A.; Kawashima, N.; Pitt, T. *Adv. Funct. Mater.* **2012**, *22*, 2735.
23. Mam, J.; Meng, Q.; Michelmore, A.; Kawashima, N.; Izzuddin, Z.; Bengtsson, C. *J. Mater. Chem.* **2013**, *1*, 4255.
24. Kango, S.; Kalia, S.; Celli, A.; Njuguna, J.; Habibi, Y.; Kumar, R. *Polym. Sci.* **2013**, *38*, 1232.
25. Hdiao, M. C.; Liao, S. H.; Yen, M. Y.; Liu, P. I.; Pu, N. W.; Wang, C. A. *ACS Appl. Mater. Interfaces* **2010**, *2*, 3092.
26. Lomeda, J. R.; Doyle, C. D.; Kosynkin, D. V.; Hwang, W.-F.; Tour, J. M. *J. Am. Chem. Soc.* **2008**, *130*, 16201.
27. Park, S.; Kim, D. S. *Polym. Eng. Sci.* **2014**, *54*, 985.
28. Lin, Z. Y.; Liu, Y.; Wong, C. P. *Langmiur* **2010**, *26*, 16110.
29. Hsiao, M. C.; Yen, M. Y.; Liu, P. I.; Pu, N. W.; Wang, C. A.; Ma, C. C. M. *ACS Appl. Mater. Interfaces* **2010**, *2*, 3092.
30. Gao, W.; Alemany1, L. B.; Ci, L.; Ajayan1, P. M. *Nat. Chem.* **2009**, *1*, 403.
31. Paredes, J. I.; Villar-Rodil, S.; Martinez-Alonso, A.; Tascon, J. M. D. *Langumuir* **2008**, *24*, 10560.
32. Guo, Y. Q.; Bao, C. L.; Song, L.; Yuan, B. H.; Hu, Y. *Ind. Eng. Chem. Res.* **2011**, *50*, 7772.
33. Liu, F.; Guo, K. *Polym. Adv. Technol.* **2014**, *25*, 418.